Haptic System Design for MRI-Guided Needle Based Prostate Brachytherapy

Hao Su* Weijian Shang Gregory A. Cole Kevin Harrington Gregory S. Fischer†

ABSTRACT

This paper presents the design of a haptic system for prostate needle brachytherapy under magnetic resonance imaging (MRI) guidance. This haptic system consists of some recently developed MRI-compatible mechatronic devices, including a fiber optic force sensor and a piezoelectric motor actuated needle driver mounted on a specifically designed 3-axis linear stage. We first propose the teleoperation framework with system architecture, infrastructure and control algorithm for the master-slave haptic interface. Then we introduce some novel sensors and actuators for MRI-compatible mechatronic devices of this haptic system. We developed the force sensor which provides in-vivo measurement of needle insertion forces to render proprioception associated with the brachytherapy procedure. We discuss the sensing principle of the optical sensor which enables two degrees-of-freedom (DOF) torque measurement and one DOF force measurement. The second apparatus of this system is a high precision 3-axis linear stage actuated by piezoelectric motors and position sensed by optical linear and rotary encoders and all of them have proved good magnetic compatibility. The needle driver can simultaneously provide needle cannula rotation and stylet translation motion while the cannula translation is engendered by the stage. The independent rotation and translation motion of the cannula and stylet can increase the targeting accuracy while minimize the tissue deformation and damage. The master-slave haptic system is capable of positioning needle and sensing insertion forces thus increasing the operation autonomy, accuracy and reducing the operation time.

Keywords: Optical Force Sensor, MRI Compatible, Haptic Feedback, Needle Driver, Prostate Needle Brachytherapy.

1 INTRODUCTION

Prostate cancer is the most common male cancer and the second most common type of cancer. Each year approximately 1.5 M core needle biopsies are performed, yielding about $220,000$ new prostate cancer cases [14]. Over $40,000$ brachytherapies are performed in the United States each year, and the number is steadily growing [6]. Transrectal ultrasound (TRUS) is the current "gold standard" for guiding both biopsy and brachytherapy due to its real-time nature, low cost, and apparent ease of use [19]. However, TRUS-guided biopsy has a detection rate of only $20\% - 30\%$ [23]. Furthermore, TRUS cannot effectively monitor the implant procedure as implanted seeds cannot be seen in the image. MRI-based medical diagnosis and treatment paradigm capitalizes on the novel benefits and capabilities created by the combination of high sensitivity for detecting tumors, high spatial resolution and high-fidelity soft tissue contrast. It seems to possess many of the capabilities that TRUS is lacking. The challenges, however, arise from the manifestation of the bidirectional MRI compatibility requirement - both the device should not disturb the scanner function and should not create image artifacts and the scanner should not disturb the device functionality [5]. Moreover, the confined physical space in closed-bore high-field MRI presents formidable challenges. Generally, the development of mechatronic devices for applications in MR environments requires meticulous consideration of safety, electromagnetic compatibility and space constraints.

A number of MRI-guided surgical procedures may be assisted through mechatronic devices that present more amiable solution than traditional manual operations due to the constraints on patient access imposed by the scanner bore. However, the lack of tactile feedback to the user limits the adoption of robotic assistants. On the other hand, the current MRI-guided biopsy procedures are performed with the patient outside the scanner bore due to the space constraint. Removing the patient from the scanner during the interventional procedure is required for most of the previously developed robotic systems. The motivation of deploying needle motion automation and haptic feedback comes from the fact that an automated robotic system with needle rotation and translation would highly increase the targeting accuracy by real-time visualization feedback and force feedback while significantly reduce the procedure duration.

A thorough review of MRI compatible systems to date for image-guided interventions by Tsekos, et al. can be found in [25]. Chinzei, et al. developed a general-purpose robotic assistant for open MRI [4] that was subsequently adapted for transperineal intraprostatic needle placement [7]. Krieger et al. presented a 2-DOF passive, un-encoded, and manually manipulated mechanical linkage to aim a needle guide for transrectal prostate biopsy with MRI guidance [16]. With the use of three active tracking coils, the device is visually servoed into position, and then, the patient is moved out of the scanner for needle insertion. Stoianovici et al. described a MR-compatible stepper motor and applied it to robotic brachytherapy seed placement [20]. This system is a fully MR-compatible, fully automatic prostate brachytherapy seed placement system; the patient is in the decubitus position and seeds are placed in the prostate transperineally. The relatively high cost and complexity of the system, in addition to the requirement to perform the procedure in a different pose than used for preoperative imaging are the major issues of this robotic platform.

Some other TRUS based robotic systems are the counterparts of the MRI compatible systems. One of the most complete robotic systems is developed by Yu and co-workers [31] and they presented the 16-DOF robotic system with 9-DOF positioning module and 7-DOF surgery module. Up to date, Fichtinger, et al. [8] developed a compact robotically assisted prostate brachytherapy system. Two parallel planar motion stages were used to position and orient the needle. More recently, [13] proposed a novel robotic brachytherapy needle-insertion system in order to replace the template used in the manual technique.

In our previous efforts, we have built an automated needle guide for MRI-guided prostate interventions that aligned the needle such that it could be inserted manually along an encoded needle guide [10]. Manual insertion was the preferred technique due to the need for tactile feedback during the insertion phase. However, it was found that the ergonomics of manual insertion along this guide

*e-mail: haosu@wpi.edu

†e-mail:gfischer@wpi.edu. Hao Su, Weijian Shang, Gregory A. Cole, Kevin Harrington and Gregory S. Fischer are with the Automation and Interventional Medicine (AIM) Laboratory in the Department of Mechanical Engineering, Worcester Polytechnic Institute, Worcester, MA, USA.

IEEE Haptics Symposium 2010
25 - 26 March, Waltham, Massachusetts, USA
978-1-4244-6820-1/10/$26.00 ©2010 IEEE

proved very difficult in the confines of the scanner bore. The limited space in closed-bore high-field MRI scanners requires a physical separation between the surgeon and the imaged region of the patient. *To overcomes the loss of needle tip proprioception information, we are developing a teleoperated haptic system with optical force-torque sensor, to be integrated with a 3-DOF robotic needle driver for MR-guided prostate needle placement.* To the authors' knowledge, [24] and [15] are the only precursors of the system framework presented here. We present a navigation and control framework with an MRI-compatible fiber optic force sensor embodiment which can be leveraged to close this measurement-control loop.

This paper is organized as follows: Section 2 describes the teleoperation framework with system architecture, infrastructure and control algorithm for the master - slave haptic interface. Section 3 describes the detailed force sensor design and prototype, linear stage design (structure, sensing and actuation) are presented in Section 4. The key contribution of this paper is the novel needle driver which is illustrated in 5. Finally, a discussion of the system is presented in Section 6.

2 Teleoperation Framework

The system architecture is based upon the robotic prostate intervention system described in [10] with major modification. An MRI compatible robot controller sits inside the scanner room and communicates to the navigation software and scanner interface running on a laptop in the console room through a fiber optic connection. However, the addition of haptic feedback modifies the architecture as demonstrated in Fig.1. The optical force sensor interface is incorporated into the in-room robot controller and the needle interaction forces are transmitted back to the navigation software console along with the robot position. We integrate the haptic feedback device into the navigation software framework to provide forces to the operator and control back to the robot.

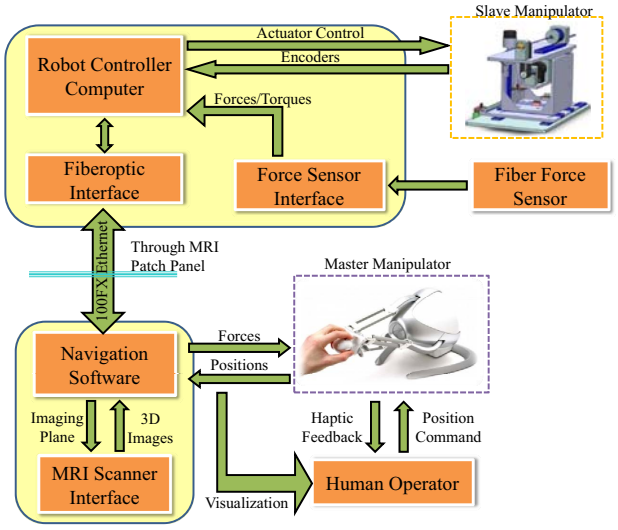

Figure 1: System architecture for the master - slave haptic interface. The fiber optic force sensor and robot are placed near the isocenter of the MRI scanner, the master manipulator is connected to the navigation software interface, and the two are couple through the robot controller in the scanner room using a fiber optic network connection.

We would like to deploy a direct force feedback architecture [3] to control the teleoperated needle placement system. In this iteration of the system, we employ a commercially available Novint Falcon (Novint Technologies, Inc., Albuquerque, NM) haptic device as the master robot. It has 3 position DOF and can be used to position the needle in the Cartesian space. The human operator positions obtained from the haptic interface are used for trajectory generation and control of the motion of the slave manipulator. The low level master control is performed by the Haptic Device Abstraction Layer provided by Novint. The slave robot in this design is the second generation of the 4-DOF robotic assistant system [10] which overcomes many design difficulties and promises safe and reliable intraprostatic needle placement inside closed high-field MRI scanners. However, the addition of force feedback allows incorporation of an actuated needle driver and firing mechanism and needle rotation. The contact forces between needle and the tissue are measured by the force/toque sensor and further fed back to the haptic device through its interface. The slave robot is shown in Fig. 3 which consists of a force sensor, a 3-DOF linear stage, and a 3-DOF needle driver.

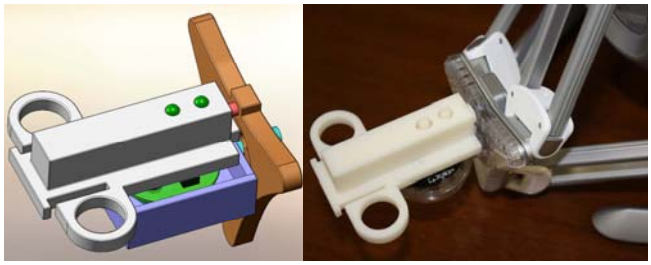

Figure 2: A model biopsy needle handle is coupled with the haptic master to mimic the sensation manual needle insertion. A CAD model of handle gripper (left) and Novint Falcon equipped with the new grip interface (right).

To get a more intuitive application of the haptic grip, we manufactured a biopsy needle like haptic gripper (a brachytherapy needle would be simpler, this biopsy needle is for illustration purpose) as shown in Fig. 2. Generally, the needle has 3-DOF Cartesian motion, while [30] indicated that continuous rotation could also be used to improve the targeting accuracy and reduce insertion force. From this perspective, we add two buttons on the top of the gripper to control the robot. In one configuration, the operator can push

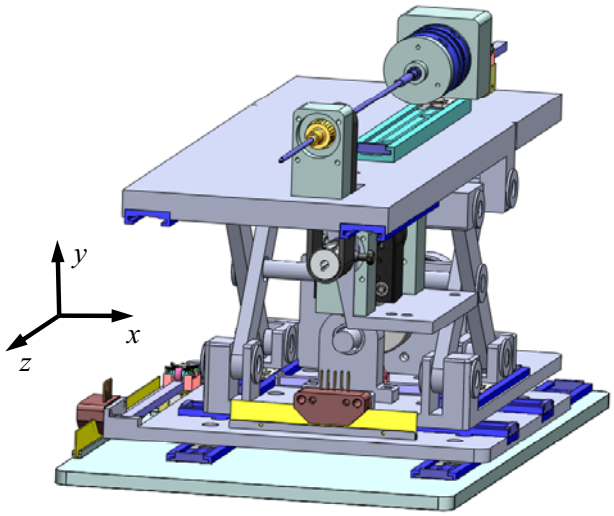

Figure 3: The slave robot consisting of a 3-DOF linear stage, force sensor and a 3-DOF needle driver.

the first button to start/stop the axial rotation of the needle cannula and the second button is used to drive the stylet translation. The de-

tailed motion control feature would be presented in Section 5. Alternatively, the buttons can be used to select targets or to constrain the needle motion to 1-DOF in the z direction when the needle is appropriately positioned in the $x-y$ plane.

3 Optical Force Sensor

Our guiding vision is to create an MRI compatible force sensor for needle-based interventional procedures by a fiber optic module with a flexible body that possesses the ability to sense needle tip interaction forces. Specifically, we intend to measure insertion force, detect tissue interfaces, and detect bone or other unexpected contact to enhance the overall clinical performance. In-vivo needle insertion force measurement is an important precursor to monitor the insertion status, consequently provides significant indicator for force sensor design. Following similar analysis of [1] by Abolhassani et. al., the needle (symmetric or asymmetric) would bend with a very small sloped deflection curve during the insertion, generically, there are 6-DOF forces/torques applied to the needle. The distributed forces orthogonal with respect to each infinitesimal segment of the needle shaft can be considered as a lumped force at the tip. The most important quantities to be sensed are the force along the needle axis and the two resultant torques of the forces tangential to the needle axes.

According to [30] and related literatures, we conclude that the force sensing range is within 15 Newton. A resolution of 0.2 Newton is sufficient in our application. The optical sensing mechanism deployed here is a economical and succinct structure which uses one spherical mirror and multiple optical fibers. A detailed design description can be found in [21] and we briefly illustrate the basic mechanism and functionality of this sensor here. The incident light emitted from a point source gets reflected by the front spherical mirror, while the reflected light can be sensed by the tip of multiple optical fibers which forms in circular pattern. The flexure converts the applied forces and torques into displacement of the mirror thus generating a light intensity change.

Fig. 4 shows the exploded view of the force sensor. The sensor has four major components: the fiber holder with eight $1mm$ diameter through holes to arrange the receiver fibers and an additional central hole for the emitter, the flexure, the spherical mirror and an adjustable mirror driver. We want the flexure to sense the axial force and lateral torques with high accuracy while tolerating off-axis forces and torques. It has two parallelogram-like segments of helical circular engravings and this structure has intrinsic axial/lateral overload protection capability. The sensor prototype is shown in Fig.5.

4 Linear Stage

To provide Cartesian positioning capability, it is very desirable to develop a generic MRI compatible linear stage. In order to satisfy

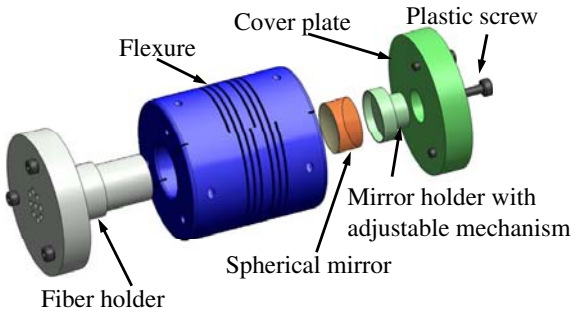

Figure 4: The exploded view of the force sensor CAD model.

Figure 5: Components of the sensor prototype with fiber guide (left),flexure (center) and cover plate with spherical mirror (right).

the close bore space limit, the linear stage dimension and workspace are specified as follows: 1) The maximum envelope dimension of the stage is $250mm$ by $150mm$ by $180mm$. The $x-y$ dimension has very confined space in the bore. 2) Horizontal translation of the base is $50mm$. 3) Vertical translation of the base: $50mm$. 4) Insertion translation of the base: $100mm$. 5) Each axis encoder positioning resolution is $0.02mm$ and the overall position accuracy should be much better than MRI pixel resolution.

A scissor mechanism actuated by a linear motor provides the vertical motion of the stage. The lead screw connection can reduce the motor capability requirement (which is critical for the friction driven piezo motion) but provide steady and high accuracy displacement. To guarantee the MRI compatibility, the linear stage is made of high strength plastics including Ultem and PEEK. The U-shaped structure can support the needle rigidly and ensure high stability. Each linear stage is constructed by DRYLIN slide and carriage (Igus, Inc., CT) which is made of anodized aluminum, a proved MRI compatible material. In order to maintain high precision of the linear stage, all three axes take advantage of piezoelectric actuators the Piezo LEGS (PiezoMotor, Uppsala, Sweden). For the horizontal motion ($x-y$ plane), we use linear piezoelectric motors and the z axis is actuated by a rotary motor which drives a lead screw to control the vertical position. The stage is shown in Fig. 3.

4.1 Encoder

Standard optical encoders (EM1-500 and E5D-1250 encoder modules with PC5 differential line driver, U.S. Digital, Vancouver, WA) have been thoroughly tested in a 3T MRI scanner for functionality and induced effects in the form of imaging artifacts, as described in [9]. The encoders have been incorporated into the robot and have performed without any stray or missed counts; the imaging artifact is confined locally to within 2 - 5 cm from the encoder. This is sufficient because the robot is designed to distance the sensors from the prostate imaging volume.

4.2 Actuator

To create the force and motion in an MR compatible system, actuators had to be selected to create the motion. For this task we selected the linear and rotary piezoelectric motor produced by PiezoMotor of Uppsala Sweden as shown in Fig. 6(a) and Fig. 6(b), for several reasons.

First, as a frictional motor capable of creating 10 N of force, when unpowered they can supply up to 16 N of holding force per motor. This acts as a safety net in this device, such that if there was a power loss the device would remain in a fixed position, and not move unpredictably. Additionally, due to the construction of the motors, multiple motors could be attached to the same drive strip, allowing us to increase the available force on a driving unit incrementally by adding more actuators to it. Fig. 6(b) shows a three motor scenario that the cascaded Piezo LEGS linear motors are used to increase the output force.

While these aspects of the motors are highly beneficial to the construction of our device there was also a serious drawback: The

(a)

(b)

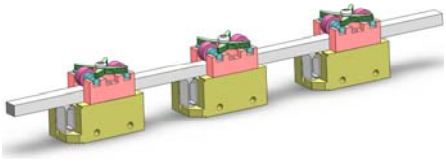

(c)

Figure 6: Piezo LEGS Linear Motor : (a) A Piezo LEGS 10 N Non-Magnetic Linear Motor, (b) A Piezo LEGS Rotary Motor 80 Nmm,(c) Three cascaded Piezo LEGS Linear Motors to increase the output force.

available driver circuitry. Piezoelectric motor drivers are typically restrictive in the types and styles of waveforms which they can supply, and often cause some image interference with a diagnostic MR imager [11]. Additionally, they are typically restrictive on how they interact with their driving control signal.

Although earlier experiments performed by Fischer and Krieger have shown piezoelectric motors to produce large amounts of interference with image quality while under motion when in their commercial off-the-shelf configuration [11], we believe that this is primarily due to lack of shielding and filtering of the drive circuits. To address these and other issues, custom driver circuits were developed for the motors, as shown in Fig. 7. The motor boards were made because available hardware to drive piezoelectric motors tends to be very expensive, and it is generally not possible to drive the motors with highly specific arbitrary waveforms. The Nanomotion single channel controller retails for close to $\$2,000$ and offers no control over the shape of the drive waveform supplied and also employs a switching power supply which may negatively affect signal integrity. The piezo driver boards we are developing will fill the need for an MR-compatible motor driver with the option of generating a highly specific arbitrary waveform. By using an embedded microcontroller, with a plurality of programmable I/Os, the user could define how the motor would be controlled by the input signals, as well as being able to design and store optimized arbitrary waveforms for the specific actuator being used. In addition to this, the output stage has been built to drive multiple motors with the same drive signal, so that if a plurality of motors are driving a single drive strip, they can be driven with the exact same signal, alleviating concerns of synchronizing the motors so they will not buck each other. An earlier version of the motor board has been tested in

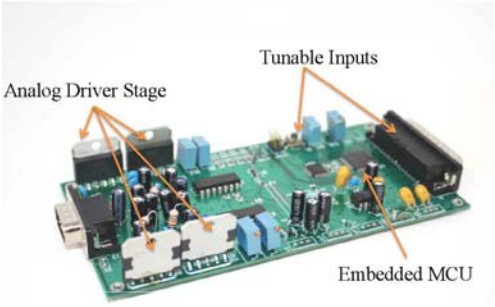

Figure 7: The piezo motor driving PCB board.

a diagnostic scanner and has been shown to not contribute a statistically detectable amount of interference with the image quality of the scanner [27].

5 Needle Driver

This section demonstrates a new needle driver that is actuated by piezoelectric motors. The needle is connected with the force sensor concentrically. And the force sensor stands on a linear slide driven by a piezoelectric motor. The resultant force by this actuation can translate the stylet along the z direction. The linear and rotary optical encoders are used to sense the needle position. To rotate the needle cannula,a timing belt which goes through the stage top plate vertically is connected with the needle clamping and the rotary motor sits beneath the top plate and is coupled with the belt with a pulley and a ceramic ball bearing. This up-down structure can significantly reduce the vertical space to fit into the scanner bore.

Rotation of the needle about its axis may be implemented to drill the needle in to limit deflection as described by Masamune, et al. [17] and Wan, et al. [26]. On the other hand, by taking advantage of the intrinsic asymmetry property of bevel needles, the needle driver may be used to steer the needle similar to traditional treatment for mobile robots and some mobile manipulators in [22]. Webster, et al. [29] explored the modeling and control of bevel steering techniques along trajectories defined using techniques described by Alterovitz et al. [2]. For different needles (brachytherapy and biopsy application), the rotation part can be the cannula for the brachytherapy needle or the whole shaft of diamond shape biopsy needle. In this design, we follow the cannula rotation approach as in [28] and [2].The most recent effort for CT compatible needle driven system is presented by Piccin, et al.[18].

The independent rotation and translation motion of the cannula and stylet can increase the targeting accuracy while minimize the tissue deformation and damage. A CAD model of the needle driver which is mounted on the top plate of the stage is shown in Fig.8 .

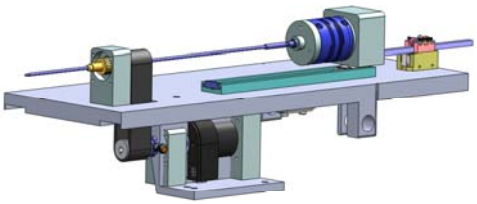

Figure 8: A CAD model of the needle driver mounted on the top plate of the stage providing cannula rotation and stylet translation motion.

To rigidly clamp the needle shaft to the driving motor mechanism, a new clamping device is developed and shown on the right of Fig.9. This mechanism is similar to a collet and a plastic screw

can be twisted to fasten the tube thus rigidly lock the clamping device on the needle shaft. The outer diameter of the clamping device is connected through a ceramic ball bearing which transmits the motor rotational motion. The clamping device is very generic in the sense that it can not only fasten brachytherapy needle but also biopsy needle instead of designing some specific structure to hold the needle handle as those in [24]. The front-rear double support fixture increase the needle rotation rigidity.

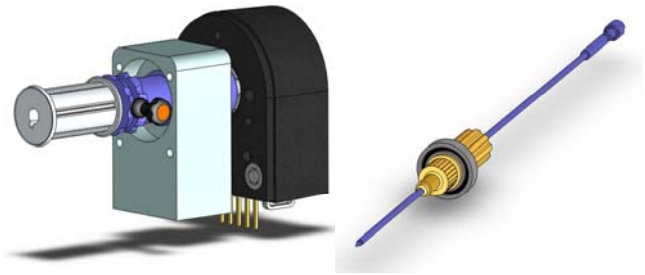

Figure 9: A detailed CAD model of the rotation stop (left) and needle clamping device (right).

To ensure surgery safety, a rotation stop that mechanically lock the rotational shaft from rotary motor is incorporated in the system in case of needle hits non-soft tissue. This mechanism is basically a push-lock structure with preloaded spring. A CAD model is shown on the left of Fig. 9 (the cover fixture is not shown). A similar stop can also be applied to the z-axis translation motion control since it is the major potential damage part.

6 Discussion

This paper presents a number of MRI-compatible haptic devices consisting of a optical force sensor, a linear stage and a new needle driver. We discussed the sensing principle of the optical sensor for in-vivo forces measurement. The 3-axis stage provides linear position capability. The needle driver can provide needle cannula rotation and stylet translation motion while the cannula translation is engendered by the 3-axis stage. The driver is actuated by piezoelectric motors and sensed by linear and rotary optical encoders. The design is able to position needle and increase the operation autonomy thus reduce the operation time. The independent rotation and translation motion of the cannula and stylet can increase the targeting accuracy while minimize the tissue deformation and damage. In addition to the target application of prostate brachytherapy and biopsy, this system can be a research platform to evaluate needle steering under real-time volumetric MR imaging.

We are in the process of incorporating all the devices and building a physical prototype to test the force feedback capability and the MRI-compatibility. The compatibility of a force sensor made of the same materials but two or three times larger in scale is validated in [12]. Further MRI scanner room tests would try to confirm the mutual compatibility of the sensor and the controller structure. Further quantitative performance experiments and results would be reported.

7 Acknowledgements

References

[1] N. Abolhassani, R. V. Patel, and F. Ayazi. Minimization of needle deflection in robot-assisted percutaneous therapy. *International Journal of Medical Robotics and Computer Assisted Surgery*, 3(2):26–34, 2007.

[2] R. Alterovitz, M. Branicky, and G. Ken. Motion planning under uncertainty for image-guided medical needle steering. *International Journal of Robotics Research*, 27(11-12):1361 – 74, 2008.

[3] M. C. Cavusoglu, A. Sherman, and F. Tendick. Design of bilateral teleoperation controllers for haptic exploration and telemanipulation of soft environments. *IEEE Transactions on Robotics and Automation*, 18(4):641 – 647, 2002.

[4] K. Chinzei, N. Hata, F. A. Jolesz, and R. Kikinis. Mri compatible surgical assist robot: System integration and preliminary feasibility study. In *MICCAI*, volume 1935, pages 921–930, October 2000.

[5] K. Chinzei and K. Miller. Towards mri guided surgical manipulator. *Med Sci Monit*, 7(1):153–163, 2001.

[6] M. R. Cooperberg, D. P. Lubeck, M. V. Meng, S. S. Mehta, and P. R. Carroll. The changing face of low-risk prostate cancer: trends in clinical presentation and primary management. *J Clin Oncol*, 22(11):2141–2149, Jun 2004.

[7] S. P. DiMaio, S. Pieper, G. Chinzei, K. Fichtinger, C. Tempany, and R. Kikinis. Robot assisted percutaneous intervention in open-mri. 18(1):11–23, Feb. 2002.

[8] G. Fichtinger, J. Fiene, C. W. Kennedy, G. Kronreif, I. I. Iordachita, D. Y. Song, E. C. Burdette, and P. Kazanzides. Robotic assistance for ultrasound guided prostate brachytherapy. *Med Image Comput Comput Assist Interv Int Conf Med Image Comput Comput Assist Interv*, 10(Pt 1):119–127, 2007.

[9] G. S. Fischer, S. P. DiMaio, I. I. Iordachita, and G. Fichtinger. Robotic assistant for transperineal prostate interventions in 3t closed mri. *Int Conf Med Image Comput Comput Assist Interv*, 10(Pt 1):425–433, 2007.

[10] G. S. Fischer, I. I. Iordachita, C. Csoma, J. Tokuda, S. P. DiMaio, C. M. Tempany, N. Hata, and G. Fichtinger. Mri-compatible pneumatic robot for transperineal prostate needle placement. *IEEE/ASME Transactions on Mechatronics*, 13(3), June 2008.

[11] G. S. Fischer, A. Krieger, I. I. Iordachita, C. Csoma, L. L. Whitcomb, and G. Fichtinger. Mri compatibility of robot actuation techniques – a comparative study. *Int Conf Med Image Comput Comput Assist Interv*, Sept. 2008.

[12] R. Gassert, D. Chapuis, H. Bleuler, and E. Burdet. Sensors for applications in magnetic resonance environments. *IEEE/ASME Transactions on Mechatronics*, 13(3):335–344, 2008.

[13] N. Hungr, J. Troccaz, N. Zemiti, and N. Tripodi. Design of an ultrasound-guided robotic brachytherapy needle-insertion system. In *Annual Conference of IEEE Engineering in Medicine and Biology Society*, pages 250–253, Minneapolis, MN, 2009.

[14] A. Jemal, R. Siegel, E. Ward, Y. Hao, J. Xu, T. Murray, and M. J. Thun. Cancer statistics, 2008. *CA Cancer J Clin*, 58(2):71–96, 2008.

[15] R. Kokes, K. Lister, R. Gullapalli, B. Zhang, A. MacMillan, H. Richard, and J. Desai. Towards a teleoperated needle driver robot with haptic feedback for rfa of breast tumors under continuous mri. *Medical Image Analysis*, 13(3):445 – 55, 2009/06/.

[16] A. Krieger, C. Csoma, I. I. Iordachital, P. Guion, A. K. Singh, G. Fichtinger, and L. L. Whitcomb. Design and preliminary accuracy studies of an mri-guided transrectal prostate intervention system. *Med Image Comput Comput Assist Interv Int Conf Med Image Comput Comput Assist Interv*, 10(Pt 2):59–67, 2007.

[17] K. Masamune, G. Fichtinger, A. Patriciu, R. C. Susil, R. H. Taylor, L. R. Kavoussi, J. H. Anderson, I. Sakuma, T. Dohi, and D. Stoianovici. System for robotically assisted percutaneous procedures with computed tomography guidance. *Comput Aided Surg*, 6(6):370–383, 2001.

[18] O. Piccin, L. Barbe, B. Bayle, M. De Mathelin, and A. Gangi. A force feedback teleoperated needle insertion device for percutaneous procedures. *International Journal of Robotics Research*, 28(9):1154 – 1168, 2009.

[19] J. C. Presti. Prostate cancer: assessment of risk using digital rectal examination, tumor grade, prostate-specific antigen, and systematic biopsy. *Radiol Clin North Am*, 38(1):49–58, Jan 2000.

[20] D. Stoianovici, D. Song, D. Petrisor, D. Ursu, D. Mazilu, M. Muntener, M. Mutener, M. Schar, and A. Patriciu. Mri stealth robot for prostate interventions. *Minim Invasive Ther Allied Technol*, 16(4):241–248, 2007.

[21] H. Su and G. Fischer. A 3-axis optical force/torque sensor for prostate needle placement in magnetic resonance imaging environments. 2nd Annual IEEE International Conference on Technologies for Practical

Robot Applications, pages 5–9, Boston, MA, USA, 2009. IEEE.

[22] H. Su and V. Krovi. Decentralized dynamic control of a nonholonomic mobile manipulator collective: A simulation study. Proceedings of the ASME Dynamic Systems and Control Conference, Ann Arbor, MI, USA, 2008.

[23] M. K. Terris, E. M. Wallen, and T. A. Stamey. Comparison of mid-lobe versus lateral systematic sextant biopsies in the detection of prostate cancer. *Urol Int*, 59(4):239–242, 1997.

[24] Z. Tse, H. Elhawary, M. Rea, I. Young, B. Davis, and M. Lamperth. A haptic unit designed for magnetic-resonance-guided biopsy. *Proceedings of the Institution of Mechanical Engineers, Part H (Journal of Engineering in Medicine)*, 223(H2):159 – 72, 2009.

[25] N. V. Tsekos, A. Khanicheh, E. Christoforou, and C. Mavroidis. Magnetic resonance-compatible robotic and mechatronics systems for image-guided interventions and rehabilitation: a review study. *Annu Rev Biomed Eng*, 9:351–387, 2007.

[26] G. Wan, Z. Wei, L. Gardi, D. B. Downey, and A. Fenster. Brachytherapy needle deflection evaluation and correction. *Med Phys*, 32(4):902–909, Apr 2005.

[27] Y. Wang, G. Cole, H. Su, J. Pilitsis, and G. Fischer. Mri compatibility evaluation of a piezoelectric actuator system for a neural interventional robot. In *Annual Conference of IEEE Engineering in Medicine and Biology Society*, pages 6072–6075, Minneapolis, MN, 2009.

[28] I. Webster, R.J., J. S. Kim, N. Cowan, G. Chirikjian, and A. Okamura. Nonholonomic modeling of needle steering. *International Journal of Robotics Research*, 25(5-6):509 – 25, 2006/05.

[29] R. J. Webster III, J. Memisevic, and A. M. Okamura. Design considerations for robotic needle steering. In *Proc. IEEE International Conference on Robotics and Automation ICRA 2005*, pages 3588–3594, 2005.

[30] Y. Yu, T. Podder, Y. Zhang, W. S. Ng, V. Misic, J. Sherman, L. Fu, D. Fuller, E. Messing, D. Rubens, J. Strang, and R. Brasacchio. Robot-assisted prostate brachytherapy. Medical Image Computing and Computer-Assisted Intervention - MICCAI 2006. 9th International Conference. Proceedings, Part I (Lecture Notes in Computer Science Vol. 4190), pages 41–9, Berlin, Germany, 2006. Springer-Verlag.

[31] Y. Yu, T. K. Podder, Y. D. Zhang, W. S. Ng, V. Misic, J. Sherman, D. Fuller, D. J. Rubens, J. G. Strang, R. A. Brasacchio, and E. M. Messing. Robotic system for prostate brachytherapy. *Comput Aided Surg*, 12(6):366–370, Nov 2007.